DMD Fast Forward. Published on July 24, 2008 as DOI: 10.1124/dmd.108.021295
DMD Fast Forward. Published on July 24, 2008 as doi:10.1124/dmd.108.021295
This article has not been copyedited and formatted. The final version may differ from this version.

DMD#21295

Enzyme Kinetics of GTI-2040, a Phosphorothioate Oligonucleotide Targeting Ribonucleotide Reductase

Xiaohui Wei,* Guowei Dai, Zhongfa Liu, Hao Cheng, Zhiliang Xie, Rebecca Klisovic, Guido Marcucci, and Kenneth K. Chan

Division of Pharmaceutics, College of Pharmacy (X.W.,G.D.,Z.L.,H.C.,Z.X.,K.K.C.), the Comprehensive Cancer Center (Z.L.,G.M.,K.K.C.), Division of Hematology-Oncology (G.M., R.K.), The Ohio State University, Columbus, OH 43210; Pharmaceutical Research Institute, Bristol-Myers-Squibb Co., Princeton, NJ 08540, USA (G.D.).

Downloaded from dmd.aspetjournals.org at ASPET Journals on April 8, 2024

Copyright 2008 by the American Society for Pharmacology and Experimental Therapeutics.

DMD Fast Forward. Published on July 24, 2008 as DOI: 10.1124/dmd.108.021295
This article has not been copyedited and formatted. The final version may differ from this version.

Running title: Enzyme kinetics of an antisense drug GTI-2040

The corresponding author: Kenneth K. Chan, Ph.D., Rm 308 OSU CCC, The Ohio State University, 410 West 12th Ave, Columbus, OH 43210, USA. Phone: 614-292-8294; FAX: 614-292-7766;

E-mail: chan.56@osu.edu

Number of text pages: 23

Number of tables: 2

Number of figures: 4

Number of references: 39

Word count: Abstract: 250

Introduction: 580

Discussion: 1086

ABBREVIATIONS: ODNs, Antisense oligonucleotides; PS-ODNs, phosphorothioate antisense oligonucleotides; GTI-2040, 5'-GGC TAA ATC GCT CCA CCA AG-3'; $CL_{int,}$ in vitro hepatic intrinsic clearance; $CL_{int,h,}$ estimated intrinsic clearance from patients; $CL_{int,h1,}$ scaled hepatic intrinsic clearance; RNR, ribonucleotide reductase; HPLC/MS/MS, high performance liquid chromatogram/tandem mass spectrometry; AML, acute myeloid leukemia; PK-PD, pharmacokinetics-pharmacodynamics; HLM, human liver microsomes; IS, internal standard; TEA, triethylamine; TEAB, triethylammonium bicarbonate; HFIP,

Downloaded from dmd.aspetjournals.org at ASPET Journals on April 8, 2024

DMD Fast Forward. Published on July 24, 2008 as DOI: 10.1124/dmd.108.021295
This article has not been copyedited and formatted. The final version may differ from this version.

1,1,1,3,3,3-hexafluoro-2-propanol; SPF, Solid Phase Extraction; MPA, mobile phase A; MPB, mobile phase B; EDTA, ethylenediamine tetraacetic acid; CL_R, renal clearance; *CrCL*, creatinine clearance; ELISA, Enzyme-Linked ImmunoSorbent Assay; PS-dC 28, 28mer polycytidine phosphorothioate oligonucleotide; SF, scaling factor; $f_{u,p}$, free fraction of GTI-2040; $f_{u(mic),}$ free fraction associated with microsomes; IRB, institution review board.

Downloaded from dmd.aspetjournals.org at ASPET Journals on April 8, 2024

DMD Fast Forward. Published on July 24, 2008 as DOI: 10.1124/dmd.108.021295
This article has not been copyedited and formatted. The final version may differ from this version.

ABSTRACT:

Enzyme kinetics of GTI-2040, a phosphorothioate ribonucleotide reductase antisense, was investigated for the first time in 3' exonuclease solution and human liver microsomes (HLM), using ion-pair HPLC method for quantification of the parent drug and two major 3'N-1 and 3'N-2 metabolites. Enzyme kinetics of GTI-2040 in 3'-exonuclease solution was found to be well characterized by Michaelis-Menten model, using the sum of formation rates of 3'N-1 and 3'N-2 (~total metabolism) because of sequential metabolism. In HLM, a biphasic binding was observed for GTI-2040 with high and low affinity constants (K_Ds) of 0.03 and 3.8 μM, respectively. Enzyme kinetics of GTI-2040 in HLM was found to deviate from Michaelis-Menten kinetics when the total GTI-2040 substrate was used. However, after correction for the unbound fractions, the formation rate of total metabolites could be described by Michaelis-Menten kinetics. Using free substrate fraction, K_m and V_{max} of GTI-2040 were determined to be 6.33 ± 3.2 μM and 16.5 ± 8.4 nmol/mg/hr, respectively. Using these values, CL_{int} in HLM was estimated to be 2.61 ± 0.56 mL/hr. The CL_{int} was then used to predict GTI-2040's *in vivo* intrinsic clearance ($CL_{int,h}$) in humans by a microsomal protein scaling factor, which gave a mean value of 182.7 L/hr, representing 24.1% of the observed *in vivo* mean $CL_{int,h1}$ of 758.7 L/hr in patients with acute myeloid leukemia. We concluded that the saturable non-specific binding of GTI-2040 in HLM complicated the interpretation of its enzyme kinetics, and scaled intrinsic clearance from HLM only partially predicted the *in vivo* intrinsic clearance.

Downloaded from dmd.aspetjournals.org at ASPET Journals on April 8, 2024

DMD Fast Forward. Published on July 24, 2008 as DOI: 10.1124/dmd.108.021295
This article has not been copyedited and formatted. The final version may differ from this version.

INTRODUCTION

Antisense oligonucleotides (ODNs) are short single strand DNA molecules designed to hybridize with specific mRNA strands thereby selectively inhibit the production of specific gene products (Stein and Cheng, 1993;Dias and Stein, 2002). This approach has been explored to target expression of genes important for malignant transformation and other pathogenetic mechanisms. For a successful therapeutic use of ODN compounds robust *in vivo* stability is critical. Previously used unmodified ODNs degraded rapidly in biological fluids by nucleases, which limited their clinical use. More recently, by substituting one of the non-bridge oxygen atoms, phosphorothioate analogs have been synthesized and shown to be more resistant to exonucleases than the unmodified ODNs (Aboul-Fadl, 2005;Crooke, 2001). Several phosphorothioate ODNs (PS-ODNs) are currently undergoing clinical evaluation for a number of diseases, including cancer, viral infections and inflammatory disorders (Marcucci et al., 2005;Crooke, 2001;Jansen and Zangemeister-Wittke, 2002). It has been reported that the *in vivo* pharmacodynamic effects of antisense correlate with the intracellular drug levels and clinical response (Dai et al., 2005a;Marcucci et al., 2005;Yu et al., 2001). Moreover, it is anticipated that a well-defined pharmacokinetics-pharmacodynamics (PK-PD) correlation may help to improve the optimization of dose regimens of PS-ODNs. As pharmacokinetics of PS-ODNs are largely driven by their disposition and metabolism (Yu et al., 2004;Crooke, 2001), it has become increasingly important to obtain a fundamental understanding of the metabolism and degradation kinetics of these compounds. Although, a significant effort has been invested in identification of the *in vivo* and *in vitro* metabolites of PS-ODNs and the 3' end

Downloaded from dmd.aspetjournals.org at ASPET Journals on April 8, 2024

DMD Fast Forward. Published on July 24, 2008 as DOI: 10.1124/dmd.108.021295
This article has not been copyedited and formatted. The final version may differ from this version.

progressively deleted metabolites mediated by the 3' exonuclease hydrolysis has been found to be the major pathway of metabolism for various PS-ODNs (Cohen et al., 1997;Crooke et al., 2000;Dai et al., 2005b;Wei et al., 2006a), few studies focusing on the enzyme kinetics of PS-ONS have been reported. In addition, it has been reported that liver is the most important organ for metabolism and disposition of PS-ODNs, although kidneys, spleen, bone marrow and lymph nodes metabolism also play a role (Butler et al., 1997;Noll et al., 2005;Cossum et al., 1993). Therefore, it is important to evaluate the contribution of hepatic metabolism to the clearance of PS-ODNs and to predict the *in vivo* CL_{int} from *in vitro* metabolism.

GTI-2040 is a 20-mer phosphorothioate oligonucleotide that inhibits the production of the R2 subunit of ribonucleotide reductase (RNR), which is essential for DNA synthesis (Lee et al., 2003). GTI-2040 has recently been shown to have promising response and acceptable tolerability in phase I clinical trials as a single agent or in combination with cytarabine for the treatment of advanced solid tumors and acute myeloid leukemia (AML) (Desai et al., 2005;Klisovic et al., 2008). Using a highly specific ion-pair HPLC/MS/MS method (Dai et al., 2005b;Gilar and Bouvier, 2000;Griffey et al., 1997), we recently reported the metabolism of GTI-2040 as the sequential nucleotide deletion via the 3' exonuclease (Wei et al., 2006). A series of progressively 3'chain-shortend metabolites were identified in several biological matrices including plasma from AML patients, solutions containing 3' exonuclease and in human liver microsomes. Herein, we investigated the enzyme kinetics of GTI-2040 in system containing either 3' exonuclease or human liver microsomes (HLM).

Downloaded from dmd.aspetjournals.org at ASPET Journals on April 8, 2024

DMD Fast Forward. Published on July 24, 2008 as DOI: 10.1124/dmd.108.021295
This article has not been copyedited and formatted. The final version may differ from this version.

Formation rates of the 3' end metabolites were monitored and used to characterize the enzyme kinetics of GTI-2040. To evaluate the contribution of liver microsomes to the metabolism of GTI-2040, the *in vitro* intrinsic clearance in HLM was determined. The *in vitro* CL_{int} was extrapolated to a predicted *in vivo* value which was compared with the intrinsic clearance determined from patients.

METHODS

Drugs and Chemicals. GTI-2040, a 20-mer phosphorothioate oligonucleotide with the sequence 5'-GGC TAA ATC GCT CCA CCA AG-3' was provided by the National Cancer Institute (Bethesda, MD) and used without further purification. Putative 3' end metabolites of GTI-2040, 3' N-1, 3' N-2, 3' N-3- GTI-2040s (here-to-fore GTI-2040 is omitted), from which 1-3 nucleotides were deleted from the 3' end, respectively, and the internal standard (IS), PS-dC 28, a 28-mer polycytidine phosphorothioate oligonucleotide were purchased from Integrated DNA Technologies (Coralville, Iowa). The purity and identity of all of the oligomers were verified by HPLC/UV/Mass spectrometry (Finnigan LCQ, San Jose, CA). Phosphodiesterase I (EC 3.1.4.1) from snake (crotalus adamanteus) venom, a 3' to 5'-exonuclease, was obtained from USB Corporation (Cleveland, OH). Pooled human liver microsomes from 18 individuals (10 males and 8 female donors) were obtained as a stock emulsion (20 mg of protein/ml in 250 mM sucrose) from BD Biosciences (Bedford, MA). HPLC-grade methanol, triethylamine (TEA, 99.5%), triethylammonium bicarbonate (TEAB) and 1,1,1,3,3,3-hexafluoro-2-propanol (HFIP, 99.8%) were purchased from Sigma-

Downloaded from dmd.aspetjournals.org at ASPET Journals on April 8, 2024

DMD Fast Forward. Published on July 24, 2008 as DOI: 10.1124/dmd.108.021295
This article has not been copyedited and formatted. The final version may differ from this version.

Aldrich Co. (St. Louis, MO). HPLC-grade water was generated by an E-pure water purification system (Barnstead, Dubuque, IA).

Sample Preparation--Solid Phase Extraction (SPE). Samples containing GTI-2040 and its metabolites were thawed and centrifuged at 1000 g for 5 min. One mL of the supernatant was mixed with 2 mL of 0.1 M TEAB and the mixture was allowed to stand at room temperature for 30 min for ion pair formation between the oligonucleotide and TEA. GTI-2040 and related metabolites were extracted with an Oasis HLB cartridge packed with 60 mg material (Waters Corp., Milford, MA). The extraction tubes were pre-conditioned with 1 mL of acetonitrile followed by 1 mL of 0.1 M TEAB (pH 8.0). Samples mixed with 0.1 M TEAB were loaded onto these pre-conditioned solid phase columns. The protein and salts were removed by sequential washings with 3 mL of 0.1 M TEAB, 3 mL of distilled water, and 3 mL of 10% acetonitrile in 0.1 M TEAB by gravity flow. Then, GTI-2040 and its related metabolites were eluted with 3 mL of 50% acetonitrile and the eluant was evaporated to dryness under N_2. The residue was reconstituted with 150 μL of Mobile Phase A and a 50 μL aliquot was analyzed by HPLC.

HPLC Conditions. Previously reported HPLC conditions (Dai et al., 2005b;Wei et al., 2006a) were used for the separation of GTI-2040 and its chain-shortened metabolites. Briefly, the separation was achieved on a 2.5 μm Waters Xterra MS18 column (50 × 2.1 mm) coupled to a MS C18 10×2.1 mm guard column (Waters Corp., Milford, MA). The mobile phase was prepared as Mobile Phase A (MPA) consisting of 100 mM HFIP buffered

Downloaded from dmd.aspetjournals.org at ASPET Journals on April 8, 2024

DMD Fast Forward. Published on July 24, 2008 as DOI: 10.1124/dmd.108.021295
This article has not been copyedited and formatted. The final version may differ from this version.

to pH 8.3 with 8.4 mM TEA and Mobile Phase B (MPB) consisting of 100 mM HFIP and 8.6 mM TEA (pH 8.3) in methanol (50:50, v/v). Gradient elution was used for the oligomer separation at a flow rate of 0.2 mL/min. The elution was initiated with 30% MPB followed by a linear increase to 45% in 30 min, and returned to 30% in 2 min, which was maintained for 8 min before the next run. The column temperature was set to 50 °C throughout the analysis using a column heater (Keystone, Woburn, MA). The autosampler temperature was kept at 4 °C throughout the sample run. A Shimadzu HPLC system consisting of two LC-10AT *vp* pumps, a SIL-10AD *vp* autosampler, and a SPD-10A *vp* UV-VIS detector was used for quantification. The detected wavelength was set at 260 nm.

Quantitation. Quantitation of metabolites was determined by comparing the formed metabolites to the control GTI-2040 at each initial concentration in the kinetic studies. Peak area ratios of GTI-2040 or each formed metabolites to the IS in each HPLC chromatogram were determined. The concentrations of formed metabolites were then calculated using the following equation:

$$C_m = \frac{R_m}{R_{G,I}} \times C_{G,I} \times \frac{E_G}{E_m} \qquad \text{Eq. 1}$$

where C_m is the concentration of the formed metabolites in the reaction medium, $C_{G,I}$ is the known concentration of control GTI-2040, R_m is the peak area ratio of metabolites to the IS, $R_{G,I}$ is the peak area ratio of control GTI-2040 to the IS, E_G and E_m are the extinction coefficients of GTI-2040 and metabolites, respectively. Concentrations of two major metabolites 3'N-1 and 3'N-2 were calculated according to Equation 1 with the $E_G/E_{m(3'N\text{-}1)}$

Downloaded from dmd.aspetjournals.org at ASPET Journals on April 8, 2024

DMD Fast Forward. Published on July 24, 2008 as DOI: 10.1124/dmd.108.021295
This article has not been copyedited and formatted. The final version may differ from this version.

ratio of 1.053 and the $E_G/E_{m(3'N-2)}$ ratio of 1.128, respectively. The other metabolites were too low to be detected and thus were not considered.

Free Drug Concentration. The extent of binding of GTI-2040 to human liver microsomes was determined by ultrafiltration method at protein concentration of 0.2 mg/mL for HLM and GTI-2040 concentration ranging between 0.1-20 μM used in the kinetic studies. EDTA (5 mM) was added to inhibit the nuclease activity in microsomes. After incubation in a 37 ºC shaking water bath for 30 min, the drug-matrix mixture was placed into a disposable Ultrafree-MC (MW cutoff 30,000) filtration system, which was centrifuged at 1500g for 30 min. An aliquot of protein-free filtrate and the initial samples were analyzed using a previously validated ELISA method (Wei et al., 2006b), which provides a low quantitation limit of 0.05 nM, and such sensitivity is required for measurement of GTI-2040 levels in ultrafiltrate. The unbound GTI-2040 fractions were estimated from the percentage of the concentrations in the filtrate compared to the initial concentrations. Samples prepared in saline were processed under the identical conditions and used as controls for non-specific binding.

Similarly, human plasma protein binding was carried out at various total drug concentrations of 1, 10, and 100 μM in donor plasma. Following incubation and centrifugation with Ultrafree-MC filtration system, an aliquot of protein-free filtrate and the initial samples were analyzed using the ELISA method. In addition, the *in vivo* free fraction of GTI-2040 in plasma ($f_{u,p}$) for AML patients was also estimated by dividing the patient's

Downloaded from dmd.aspetjournals.org at ASPET Journals on April 8, 2024

DMD Fast Forward. Published on July 24, 2008 as DOI: 10.1124/dmd.108.021295
This article has not been copyedited and formatted. The final version may differ from this version.

renal clearance (CL_R) with the glomerular filtration rate, which is estimated by patient's creatinine clearance (*CrCL*) (Rowland and Tozer, 1995):

$$f_{u,p} = \frac{CL_R}{CrCL}. \quad \text{Eq. 2}$$

CL_R for each patient was determined in Equation 8 (shown later).

Enzyme Kinetics of GTI-2040 in the Solution Containing 3' Exonuclease. To prepare the 10 U/ml stock solution of Phosphodiesterase I, the lyophilized enzyme was reconstituted in Tris-salt buffer:glycerol (50:50, v/v) containing 110 mM Tris-HCl, pH 8.9, 110 mM NaCl, 15 mM $MgCl_2$, and stored at –20 °C before use. To conduct the enzyme kinetic study, various concentrations of GTI-2040 ranging from 0.1 to 20 μM were incubated with 0.3 U/ml of Phosphodiesterase I diluted in MPA (100 mM HFIP titrated to pH 8.3 by 8.4 mM TEA) at 37 °C for 0.5 hr. This specific condition is required for the HPLC assay as the typically used buffer system was found to interfere with the separation of GTI-2040 and its metabolites. The reaction matrix has previously shown to possess similar metabolic activity as in the buffer (Wei et al., 2006a) . The incubation time and quantity of enzyme used were both within the linear region in the reaction condition. The reactions were terminated by the addition of 5 mM EDTA. Then, an appropriate amount of PS-dC 28 was added and used as the internal standard and the samples were immediately frozen until analysis. For analysis, samples were thawed at 4 °C and analyzed by HPLC without further preparation. Solutions spiked with the known initial levels of GTI-2040 in 0.3 U/ml Phosphodiesterase I containing appropriate amounts of PS-dC 28 and 5 mM EDTA without enzyme reaction were prepared as GTI-2040 controls for the calculation of metabolite concentration.

Downloaded from dmd.aspetjournals.org at ASPET Journals on April 8, 2024

DMD Fast Forward. Published on July 24, 2008 as DOI: 10.1124/dmd.108.021295
This article has not been copyedited and formatted. The final version may differ from this version.

Enzyme Kinetics of GTI-2040 in Pooled Human Liver Microsomes. Incubations of GTI- 2040 were carried out under initial linear conditions with respect to time (30 min) and microsomal protein concentration (0.2 mg protein/mL). This protein concentration was selected based on the best linear condition from evaluation of 0.1, 0.2, and 0.5 mg/mL. Substrates at the concentration range between 0.1 and 20 μM were incubated with human liver microsomes in a 1 mL tube in a shaking water bath at 37 °C with frequent inversed mixing. All incubations were performed in duplicate. At the end of incubation, 5 mM EDTA was added to stop the reaction. Appropriate amounts of the IS PS-dC 28 were added into each sample. The mixture was then centrifuged at 3000 g for 2 min and the supernatant was separated and stored at –80 °C until analysis. GTI-2040 and its metabolites were extracted with SPE and analyzed by HPLC-UV. Another set of EDTA treated HLM samples containing GTI-2040 at initial concentrations and PS-dC 28 without incubation was carried out with the extraction as described as above and was used as the control GTI-2040 for the calculation of the metabolite concentration.

Clinical studies. A National Cancer Institute (NCI)/Cancer Therapy Evaluation Program (CTEP)–sponsored phase I clinical trial of GTI-2040 in patients with refractory or relapsed AML was carried out at the Ohio State University James Cancer Hospital and Research Institute in adherence to the Institute Research Review Board (IRB). Informed consent was obtained before entry onto the study.

Downloaded from dmd.aspetjournals.org at ASPET Journals on April 8, 2024

DMD Fast Forward. Published on July 24, 2008 as DOI: 10.1124/dmd.108.021295
This article has not been copyedited and formatted. The final version may differ from this version.

***In vivo* Clearance.** Patients with AML were treated with GTI-2040 at 3.5 or 5 mg/kg/day as a continuous i.v. infusion for a total of 144 hr. Blood was drawn at various time points during and post infusion. Plasma was separated from the whole blood by centrifugation at 1400g for 20 min. Pretreatment and 24 hr cumulative urine was also collected. GTI-2040 concentrations in plasma and urine were determined by the previously reported ELISA method (Dai et al., 2005a;Wei et al., 2006b).

Non-specific binding in HLM. The non-specific binding of GTI-2040 in HLM is described by Eq. 3. K_D and B_{max} were calculated from the Scatchard equation (Eq. 4), which is a linear transformation of Eq. 3.

$$C_B = \frac{B_{\max} \times C_F}{K_D + C_F} \quad \text{Eq. 3}$$

$$\frac{C_B}{C_F} = \frac{B_{\max}}{K_D} - \frac{C_B}{K_D} \quad \text{Eq.4}$$

where C_B is the concentration of the bound drug in HLM, C_F is the free drug concentration in HLM, B_{max} is the maximal binding capacity and K_D is the binding dissociation constant.

Calculation of the *in vitro* CL_{int}. The rate-substrate concentration profiles were fitted by the Michaelis-Menten equation (Eq. 5) or Hill equation (Eq. 6) using the non-linear regression model in SigmaPlot (Systat Inc., Point Richmond, CA).

$$v = \frac{V_{\max} \times S}{K_m + S} \quad \text{Eq. 5}$$

Downloaded from dmd.aspetjournals.org at ASPET Journals on April 8, 2024

DMD Fast Forward. Published on July 24, 2008 as DOI: 10.1124/dmd.108.021295
This article has not been copyedited and formatted. The final version may differ from this version.

$$v = \frac{V_{\max} \times S^n}{S_{50}^n + S^n} \qquad \text{Eq. 6}$$

where v and $V_{\max}$ are the observed and maximal rates of metabolism, K_m is Michaelis constant and is the concentration at half of $V_{\max}$ in the Michaelis-Menten equation, S_{50} is the concentration at half of $V_{\max}$ in the Hill equation, n is the Hill coefficient, and S is the unbound substrate concentration. The *in vitro* CL_{int} was then estimated from Equations 7.

$$\textit{in vitro} \quad CL_{\text{int}} = \frac{V_{\max}}{K_m} \qquad \text{Eq. 7}$$

Calculation of the *in vivo* $CL_{int,h}$ from patients. Renal clearance of GTI-2040 in patients was estimated by dividing the cumulative amount of GTI-2040 in 24 hr urine to the 24 hr plasma AUC, as shown in Equation 9. Assuming that the total clearance for GTI-2040 consists of mainly renal and hepatic clearances and only minimal parent drugs would undergo biliary excretion (Lischda et al.,2003), the hepatic clearance from patients can therefore be obtained by subtracting renal clearance from the total plasma clearance (Equation 10).

$$CL_R = \frac{A_{urine0-24hr}}{AUC_{plasma0-24hr}} \qquad \text{Eq. 8}$$

$$CL_H = CL - CL_R \qquad \text{Eq. 9}$$

CL_H is given by the following equation:

$$CL_H = \frac{Q_H \times f_{u,p} \times CL_{\text{int},h}}{Q_H + f_{u,p} \times CL_{\text{int},h}} \qquad \text{Eq. 10}$$

which can be transformed into

Downloaded from dmd.aspetjournals.org at ASPET Journals on April 8, 2024

DMD Fast Forward. Published on July 24, 2008 as DOI: 10.1124/dmd.108.021295
This article has not been copyedited and formatted. The final version may differ from this version.

$$in\ vivo\ CL_{\text{int},h} = \frac{CL_H}{f_{u,p}(1-\frac{CL_H}{Q_H})} \qquad \text{Eq. 11}$$

where $f_{u,p}$ is the free fraction of the drug in plasma and was determined from Equation 2. $CL_{\text{int,h}}$ is the in vivo intrinsic clearance estimated in patients. Q_H is the hepatic plasma flow rate and was estimated to be 49 liters/hr for a 70-kg human.

Scaling of the *in vitro* CL_{int} to the *in vivo* $CL_{\text{int,h1}}$. Microsomal protein amount was used as a scaling factor to transform the *in vitro* CL_{int} in microsomes to the *in vivo* $CL_{\text{int,h1}}$ value. Assuming that 1 g of liver contains approximately 50 mg of microsomal protein and the liver of a 70-kg human weighs approximately 1,400 g, a scaling factor (SF) of 70,000 mg is obtained (Kuhnz and Gieschen, 1998). Multiplication of the *in vitro* CL_{int} by this scaling factor yields the scaled *in vivo* $CL_{\text{int,h1}}$, expressed as liters per hour.

$$\text{Scaled } in\ vivo\ \text{CL}_{\text{int,h1}} = \text{SF} \times in\ vitro\ CL_{\text{int}} \qquad \text{Eq. 12}$$

RESULTS

Protein binding. In human plasma, GTI-2040 was found to exhibit concentration-dependent high plasma protein binding. At total GTI-2040 concentrations of 0.5, 1, 10, 100 μM, mean free drug fractions were found to be 0.05%, 0.09, 2.2% and 5.5%, respectively (Table 1). When plasma total GTI-2040 concentration was <0.5 μM, free drug concentrations in the ultrafiltrate fell below the LLOQ (0.05 nM) of the ELISA assay. Since

Downloaded from dmd.aspetjournals.org at ASPET Journals on April 8, 2024

DMD Fast Forward. Published on July 24, 2008 as DOI: 10.1124/dmd.108.021295
This article has not been copyedited and formatted. The final version may differ from this version.

most of the clinically relevant plasma GTI-2040 concentrations are at about 0.5 μM (ranging from 0.114 μM to 0.728 μM), it is technically difficult to determine the free drug concentration by ultrafiltration method. In order to obtain an assessment of the free fraction of drug in patients ($f_{u,p}$), the *in vivo* $f_{u,p}$ for GTI-2040 was estimated by the ratio of patients renal clearance to the corresponding creatinine clearance and was found to be in the range between 0.0034% and 0.256% with a mean value of 0.071% in 21 patients. This result is in the same range as estimated by extrapolation from the in vitro protein-binding as described above.

In HLM, a concentration-dependent binding of GTI-2040 was observed as shown in Table 1 and Figure 1. When GTI-2040 concentrations were increased from 0.1 μM to 20 μM, the free fraction of GTI-2040 in HLM (0.2 mg protein/mL) was found to increase from 7.2 % to 63.9 %. As shown in Figure 1A, the binding appears to be saturated when the substrate concentrations were higher than 10 μM. Two straight lines with different slopes were obtained from the Scatchard plots (Figure 1B), indicating that more than one binding site were present with different affinities in HLM for GTI-2040. A higher binding affinity with a binding dissociation constant K_D = 0.03 μM, and a maximum binding capacity B_{max}=0.49 μM and a lower binding affinity with K_D = 3.8 μM and B_{max}=8.9 μM were calculated from the Scatchard equation (Eq.4).

Downloaded from dmd.aspetjournals.org at ASPET Journals on April 8, 2024

DMD Fast Forward. Published on July 24, 2008 as DOI: 10.1124/dmd.108.021295
This article has not been copyedited and formatted. The final version may differ from this version.

Kinetics of Metabolite Formation of GTI-2040 in 3' Exonuclease Solution. Using the HPLC method, GTI-2040 and its 3' chain-shortened metabolites derived from Phosphodiesterase I were well separated (data not shown). At the incubation period of 0.5 hr, 3'N-1 and 3'N-2 were found to be the two major metabolites in all evaluated substrate concentrations. The dose recoveries, calculated as the sum of percentage of parent and metabolites (3'N-1 and 3'N-2) to the added amounts of GTI-2040, were found to be in the range of 85.8-109.8% (mean 98.8%) over the substrate level from 0.1 to 20 μM, indicating that the sum of 3'N-1 and 3'N-2 essentially accounts for the total metabolism of GTI-2040 during the initial incubation period.

Since metabolism of GTI-2040 was found mainly through sequential deletion of a single 3' end nucleotide, enzyme kinetics of GTI-2040 in 0.3 U/ml of Phosphodiesterase I was evaluated using the sum of the formation rates of 3'N-1 and 3'N-2 metabolites (representing nearly total metabolism) and the results are presented in Figures 2A and 2B. As shown in Figure 2A, a hyperbolic saturation curve was observed, and when transformed to the Eadie-Hofstee format, a linear plot was observed (Figure 2B), conforming to the Michaelis-Menten kinetics. Therefore the Michaelis-Menten equation was used to fit the formation kinetics of total metabolites. As determined by Eq. 5, the K_m was found to be 1.28 ± 0.42 μM and the V_{max} 0.73 ± 0.06 nmol/hr. CL_{int} of GTI-2040 in 0.3 U/ml of Phosphodiesterase I, as the ratio of V_{max} to K_m, was calculated to be 0.60 ± 0.19 mL/hr. The estimated kinetic constants are listed in Table 2.

Downloaded from dmd.aspetjournals.org at ASPET Journals on April 8, 2024

DMD Fast Forward. Published on July 24, 2008 as DOI: 10.1124/dmd.108.021295
This article has not been copyedited and formatted. The final version may differ from this version.

Kinetics of Metabolites Formation of GTI-2040 in Pooled Human Liver Microsomes. GTI-2040 and its metabolites from HLM incubation were well separated using the ion-pair HPLC system and no interference was found from the control HLM (data not shown). In the initial incubation period of 0.5 hr, 3'N-1 and 3'N-2 were found to be the major metabolites in all of the tested substrate concentrations. The drug recoveries were estimated by comparison of the sum of the unchanged GTI-2040 and metabolites to the added amount of GTI-2040 and found to be in the range of 89.6-110.0% with a mean value of 98.9% over the substrate concentrations from 0.1 to 20 μM, indicating that the sum of 3'N-1 and 3'N-2 essentially accounts for the total metabolism of GTI-2040 in HLM during the initial incubation period.

The sum of the formation rates of the major metabolites 3'N-1 and 3'N-2 was plotted against the total substrate GTI-2040 concentrations and a sigmoidal shape curve is shown in Figure 3A. These data were reprocessed using an Eadie-Hofstee plot as shown in Figure 3B. The Eadie-Hofstee plot exhibits a curvilinear curve instead of a commonly found straight line. A curved Eadie-Hofstee plot indicates deviation from the classical Michaelis-Menten model (Houston and Kenworthy, 2000;Houston and Galetin, 2005;Tracy, 2006). In this case, the Hill equation (Eq. 6) is commonly used for estimation of the parameters for the compound displaying atypical kinetics and the S_{50} was calculated to be 12.1 ± 8.6 μM, the Vmax 16.8 ± 8.0 nmol/hr/mg proteins, and the Hill coefficient 1.28 ± 0.4. The relevant kinetic constants as estimated are listed in Table 2. Since the metabolic system in HLM contains microsomal membrane, to examine the impact of the non-specific binding of GTI-

Downloaded from dmd.aspetjournals.org at ASPET Journals on April 8, 2024

DMD Fast Forward. Published on July 24, 2008 as DOI: 10.1124/dmd.108.021295
This article has not been copyedited and formatted. The final version may differ from this version.

2040 in HLM on the enzyme kinetic curves, free fraction of GTI-2040 in HLM was employed to calculate the formation rate of metabolites (Figure 4A). As shown in Figure 4B, the Eadie-Hofstee plots shows a linear trend using the free concentrations of substrate in the range from 0.0159 to 12.8 μM (corresponding to 0.1 to 20 μM of total drug concentrations). Metabolism kinetics of GTI-2040 in HLM was fitted with a Michaelis-Menten model, and Eq. 5 was used to calculate the kinetic rate constants. As listed in Table 2, after correcting with the free fraction of the substrate, the K_m was estimated to be 6.33 ± 3.2 μM, the V_{max} was 16.5 ± 8.4 nmol/hr/mg protein, and the CL_{int} (V_{max}/K_m) was 2.61 ± 0.56 mL/hr.

Correlation of the *in vitro* CL_{int} from HLM with the *In vivo* $CL_{int,h}$. Renal clearance from 21 AML patients was determined to be in the range between 0.00026 and 0.019 L/hr with a mean value of 0.0032 L/hr. Following Equations 9-11, the *in vivo* intrinsic clearance was found to vary from 238.7 L/hr to 2846.4 L/hr with a mean value at 758.7 L/hr. Since it is the unbound drug that gains access to the active site of metabolic enzymes, the *in vitro* HLM CL_{int} that calculated from the unbound GTI-2040 substrate concentrations was used to estimate the *in vivo* $CL_{int,h1}$ using the microsomal protein scaling factor (Eq. 12). In this fashion, the predicted *in vivo* $CL_{int,h1}$ was determined to be 182.7 L/hr which represented 24.1% of the observed $CL_{int,h}$ in patients. Detailed clinical pharmacokinetics of GTI 2040 in AML patients has recently been published (Klisovic et al., 2008).

Downloaded from dmd.aspetjournals.org at ASPET Journals on April 8, 2024

DMD Fast Forward. Published on July 24, 2008 as DOI: 10.1124/dmd.108.021295
This article has not been copyedited and formatted. The final version may differ from this version.

DISCUSSION

In this study, enzyme kinetics of GTI-2040 was characterized as its metabolites formation rate in both pure enzyme solution and human liver microsomes. In 3' exonuclease solution system, where protein binding is negligible, the formation rate of sum of 3'N-1 and 3'N-2, two main GTI-2040 metabolites, was well fitted with Michaelis-Menten model (Figures 2A and 2B). Since the metabolism of GTI-2040 has been found to mainly undergo sequential nucleotide deletion via 3' exonuclease, it is important to take into account of its sequential metabolism in order to correctly interpret its enzyme kinetics. When only the 3'N-1 metabolite was considered as the sole pathway, the Eadie-Hofstee plot is nonlinear in the range of evaluated substrate concentrations and the enzyme kinetics deviates from Michaelis-Menten model as a result of underestimation of the extent of metabolism (data not shown). However, when the sum of 3'N-1 and 3'N-2 metabolites was taken into account, the Eadie-Hofstee plot became linear and the kinetics appeared to follow the Michaelis-Menten model. Since in this tested metabolism system, >85% dose of GTI-2040 was accounted for by the measurement of the sum of GTI-2040 and the 3'N-1 and 3'N-2 metabolites under the initial reaction condition, therefore the use of sum of 3'N-1 and 3'N-2 metabolites should correctly describe the enzyme kinetics of GTI-2040 in the 3' exonuclease solution.

When enzyme kinetics of GTI-2040 in HLM was analyzed using the sum of the formation rate of 3'N-1 and 3'N-2, a sigmoidal kinetics of GTI-2040 was observed and a curvilinear Eadie-Hofstee plot was obtained (Figures 3A and 3B). This would suggest an enzyme

Downloaded from dmd.aspetjournals.org at ASPET Journals on April 8, 2024

DMD Fast Forward. Published on July 24, 2008 as DOI: 10.1124/dmd.108.021295
This article has not been copyedited and formatted. The final version may differ from this version.

autoactivation by the substrate (Houston and Kenworthy, 2000; Tracy, 2006) and in such a case a Hill equation may have to be used for enzyme kinetic analysis. However, after the formation rate of total metabolites was corrected using the free fractions of substrate GTI-2040 at each concentration level, an apparent, normal Michaelis-Menten plot, but a biphasic Eadie-Hofstee plot composed of two linear segments approximately above and below an unbound substrate concentration of about 0.112 μM (equivalent to total substrate concentration at 0.5 μM) was shown (Figure 4B). This biphasic Eadie-Hofstee plot might relate to our previous Scatchard analysis (Figure 1, Table 1), which shows two binding sites with rather different binding dissociate constants, as the slope of the Eadie-Hofstee plot reflects the Km of GTI-2040 to the HLM. This renders the enzyme kinetics analysis rather complex in HLM, if both binding sites are included. For example, if the fraction of unbound drug in HLM ($f_{u(mic)}$) is constant over the range of substrate concentrations, the apparent $K_{m,app}$ value is usually converted to the free K_m by multiplication of $f_{u(mic)}$ (Tang et al., 2002;Isoherranen et al., 2004). However, if the binding is concentration dependent and the substrate concentration range used (the determined K_m value as well) is similar to or higher than the K_D, fractions of the unbound drug ($f_{u(mic)}$) may vary over the substrate concentration range used and free Km value cannot be calculated from a constant $f_{u(mic)}$. Then, in such a case sigmoidal kinetics and curvilinear Eadie-Hofstee plots could arise as a consequence to the various free fractions of the substrate available to the enzyme (McLure et al., 2000;Houston and Kenworthy, 2000). Thus, the sigmoidal kinetics of GTI-2040 observed for HLM may be due to, in part, a concentration-dependent binding to microsomal membrane.

Downloaded from dmd.aspetjournals.org at ASPET Journals on April 8, 2024

DMD Fast Forward. Published on July 24, 2008 as DOI: 10.1124/dmd.108.021295
This article has not been copyedited and formatted. The final version may differ from this version.

Since it is the unbound drugs that become available to interact with enzyme, the unbound substrate concentrations mostly fell below the binding dissociation constants to the HLM and the Km for the 3'-exonuclease of 1.28 μM, we elected to approximate the enzyme kinetics in the HLM using the Michaelis-Menton Model. Additionally, clinically GTI-2040 is used as a 6 day infusion and the total steady-state concentrations are in the range of 0.3 μM (Klisovic et al., 2008), further justifying the use of the apparent Michaelis-Menten kinetics to describe the GTI-2040 data for approximation of the HLM enzyme kinetics, which yielded the kinetic parameter as shown in Table 2. Notably, the Km value was determined to be 6.33 μM, using the unbound substrate concentrations and this value is greater than both K_D values of GTI-2040 in HLM. This approximation is especially relevant clinically, as the steady-state drug concentrations seen in circultation were well above 0.1 μM (Klisovic et al., 2008) and would be adequate to estimate the *in vitro* intrinsic clearance of GTI-2040 in HLM, which allows for the *in vitro*-*in vivo* correlation.

In vivo intrinsic clearance from patients was compared to the predicted $CL_{int,h1}$ that was scaled up from the CL_{int} in HLM. The predicted *in vivo* $CL_{int,h1}$ accounted for 24.1% of the observed *in vivo* $CL_{int,h}$. This might indicate that human liver microsomes only partially contributed to the metabolism of GTI-2040. The underestimation of the *in vivo* $CL_{int,h1}$ is likely due to the multiple metabolism sites of PS-ODNs *in vivo*. *In vivo*, PS-ODNs extensively distribute to different organs and tissues with the majority of drugs accumulating within the liver and the kidneys (Griffey et al., 1997;Noll, McCluskie et al.,

Downloaded from dmd.aspetjournals.org at ASPET Journals on April 8, 2024

DMD Fast Forward. Published on July 24, 2008 as DOI: 10.1124/dmd.108.021295
This article has not been copyedited and formatted. The final version may differ from this version.

2005;Yu et al., 2004;Agrawal et al., 1991). In the liver, PS-ODNs are not only taken up into the hepatocytes but also rapidly distributes to the nonparenchymal cells, including Kupffer cells and endothelial cells (Nolting et al., 1997;Graham et al., 2001), and only small amount of drug is excreted into the bile (Lischka et al., 2003). In addition to the liver, kidneys are another important organ responsible for the degradation of PS-ODN. Significant amounts of chain-shortened metabolites were detected in the kidneys, especially in the proximal tubular cells (Griffey et al., 1997;Noll et al., 2005). Metabolism of GTI-2040 and other PS-ODNs was also found in circulation and other organ tissues in addition to liver (Gilar et al., 1997;Wei et al., 2006a). Therefore, liver microsomes may not be the sole responsible system for the full prediction of the *in vivo* metabolism of GTI-2040. In addition, it is reported that *in vivo* human intrinsic clearance is usually under-predicted using human liver microsomes possibly due to the variability of the source of liver donated (Brown et al., 2007). The current predicted value is considered not unreasonable relative to other drugs.

This is the first time that enzyme kinetics study of GTI-2040 was investigated in a pure enzyme solution and in human liver microsomes. It is interesting to observe sigmoidal kinetics of GTI-2040 in HLM, which we attributed to the complex effects such as the sequential metabolism and the saturable non-specific binding in HLM. Whether this phenomenon applies to other PS-ODNs remains to be demonstrated. Nevertheless, our studies suggest that careful interpretation of the enzyme kinetics of PS-ODNs, with respect to the presence of sequential metabolism, high protein binding, and the saturable non-

Downloaded from dmd.aspetjournals.org at ASPET Journals on April 8, 2024

DMD Fast Forward. Published on July 24, 2008 as DOI: 10.1124/dmd.108.021295
This article has not been copyedited and formatted. The final version may differ from this version.

specific binding in the metabolism systems should be made. In addition, we have found that the scaled intrinsic clearance from the *in vitro* HLM represented 24.1% of GTI-2040 *in vivo* intrinsic clearance from AML patients probably is due to the partial contribution of liver microsomes in metabolism of GTI-2040.

Downloaded from dmd.aspetjournals.org at ASPET Journals on April 8, 2024

DMD Fast Forward. Published on July 24, 2008 as DOI: 10.1124/dmd.108.021295
This article has not been copyedited and formatted. The final version may differ from this version.

REFERENCE

Aboul-Fadl T (2005) Antisense oligonucleotides: the state of the art. *Curr.Med.Chem.* **12**:2193-2214.

Agrawal S, Temsamani J, and Tang JY (1991) Pharmacokinetics, biodistribution, and stability of oligodeoxynucleotide phosphorothioates in mice. *Proc.Natl.Acad.Sci.U.S.A* **88**:7595-7599.

Brown HS, Griffin M, and Houston JB (2007) Evaluation of cryopreserved human hepatocytes as an alternative in vitro system to microsomes for the prediction of metabolic clearance. *Drug Metab Dispos.* **35**:293-301.

Butler M, Stecker K, and Bennett CF (1997) Cellular distribution of phosphorothioate oligodeoxynucleotides in normal rodent tissues. *Lab Invest* **77**:379-388.

Cohen AS, Bourque AJ, Wang BH, Smisek DL, and Belenky A (1997) A nonradioisotope approach to study the in vivo metabolism of phosphorothioate oligonucleotides. *Antisense Nucleic Acid Drug Dev.* **7**:13-22.

Cornish-Bowden Athel (1995) Introduction to enzyme kinetics, in *Fundamental of enzyme kinetics* pp 16-37, London : Portland.

Cossum PA, Sasmor H, Dellinger D, Truong L, Cummins L, Owens SR, Markham PM, Shea JP, and Crooke S (1993) Disposition of the 14C-labeled phosphorothioate oligonucleotide ISIS 2105 after intravenous administration to rats. *J.Pharmacol.Exp.Ther.* **267**:1181-1190.

Crooke ST. Antisense Drug Technology. Richard S Geary, Rosie Z.Yu, Janet M.Leeds, Tanya A.Watanabe, Scott P.Henry, and Arthur A.Levin. Pharmacokinetic properties in animals. 139-141. 2001.
Ref Type: Generic

Crooke RM, Graham MJ, Martin MJ, Lemonidis KM, Wyrzykiewiecz T, and Cummins LL (2000) Metabolism of antisense oligonucleotides in rat liver homogenates. *J.Pharmacol.Exp.Ther.* **292**:140-149.

Dai G, Chan KK, Liu S, Hoyt D, Whitman S, Klisovic M, Shen T, Caligiuri MA, Byrd J, Grever M, and Marcucci G (2005a) Cellular uptake and intracellular levels of the bcl-2 antisense g3139 in cultured cells and treated patients with acute myeloid leukemia. *Clin.Cancer Res.* **11**:2998-3008.

Downloaded from dmd.aspetjournals.org at ASPET Journals on April 8, 2024

DMD Fast Forward. Published on July 24, 2008 as DOI: 10.1124/dmd.108.021295
This article has not been copyedited and formatted. The final version may differ from this version.

Dai G, Wei X, Liu Z, Liu S, Marcucci G, and Chan KK (2005b) Characterization and quantification of Bcl-2 antisense G3139 and metabolites in plasma and urine by ion-pair reversed phase HPLC coupled with electrospray ion-trap mass spectrometry. *J.Chromatogr.B Analyt.Technol.Biomed.Life Sci.* **825**:201-213.

Desai AA, Schilsky RL, Young A, Janisch L, Stadler WM, Vogelzang NJ, Cadden S, Wright JA, and Ratain MJ (2005) A phase I study of antisense oligonucleotide GTI-2040 given by continuous intravenous infusion in patients with advanced solid tumors. *Ann.Oncol.* **16**:958-965.

Dias N and Stein CA (2002) Antisense oligonucleotides: basic concepts and mechanisms. *Mol.Cancer Ther.* **1**:347-355.

Emoto C, Yamazaki H, Iketaki H, Yamasaki S, Satoh T, Shimizu R, Suzuki S, Shimada N, Nakajima M, and Yokoi T (2001) Cooperativity of alpha-naphthoflavone in cytochrome P450 3A-dependent drug oxidation activities in hepatic and intestinal microsomes from mouse and human. *Xenobiotica* **31**:265-275.

Gilar M, Belenky A, Smisek DL, Bourque A, and Cohen AS (1997) Kinetics of phosphorothioate oligonucleotide metabolism in biological fluids. *Nucleic Acids Res.* **25**:3615-3620.

Gilar M and Bouvier ESP (2000) Purification of crude DNA oligonucleotides by solid-phase extraction and reversed-phase high-performance liquid chromatography. *J.Chromatogr.A* **890**:167-177.

Graham MJ, Crooke ST, Lemonidis KM, Gaus HJ, Templin MV, and Crooke RM (2001) Hepatic distribution of a phosphorothioate oligodeoxynucleotide within rodents following intravenous administration. *Biochem.Pharmacol.* **62**:297-306.

Griffey RH, Greig MJ, Gaus HJ, Liu K, Monteith D, Winniman M, and Cummins LL (1997) Characterization of oligonucleotide metabolism in vivo via liquid chromatography/electrospray tandem mass spectrometry with a quadrupole ion trap mass spectrometer. *J.Mass Spectrom.* **32**:305-313.

Harlow GR and Halpert JR (1998) Analysis of human cytochrome P450 3A4 cooperativity: construction and characterization of a site-directed mutant that displays hyperbolic steroid hydroxylation kinetics. *Proc.Natl.Acad.Sci.U.S.A* **95**:6636-6641.

Houston JB and Galetin A (2005) Modelling atypical CYP3A4 kinetics: principles and pragmatism. *Arch.Biochem.Biophys.* **433**:351-360.

Houston JB and Kenworthy KE (2000) In vitro-in vivo scaling of CYP kinetic data not consistent with the classical Michaelis-Menten model. *Drug Metab Dispos.* **28**:246-254.

Downloaded from dmd.aspetjournals.org at ASPET Journals on April 8, 2024

DMD Fast Forward. Published on July 24, 2008 as DOI: 10.1124/dmd.108.021295
This article has not been copyedited and formatted. The final version may differ from this version.

Isoherranen N, Kunze KL, Allen KE, Nelson WL, and Thummel KE (2004) Role of itraconazole metabolites in CYP3A4 inhibition. *Drug Metab Dispos.* **32**:1121-1131.

Jansen B and Zangemeister-Wittke U (2002) Antisense therapy for cancer--the time of truth. *Lancet Oncol.* **3**:672-683.

Kenworthy KE, Clarke SE, Andrews J, and Houston JB (2001) Multisite kinetic models for CYP3A4: simultaneous activation and inhibition of diazepam and testosterone metabolism. *Drug Metab Dispos.* **29**:1644-1651.

Klisovic R, Blum W, Wei X, Liu S, Liu Z, Xie Z, Vukosavljevic T, Kafauver C, Huynh L, Pang J, Zwiebel J, Devine S, Byrd J, Grever M, Chan K, and Marcucci G (2008) Phase I study of GTI-2040, an anti-sense to ribonucleotide reductase, in combination with high dose cytarabine in patients with acute myeloid leukemia. *Clin.Cancer Res.***14**: 3889-3895.

Kuhnz W and Gieschen H (1998) Predicting the oral bioavailability of 19-nortestosterone progestins in vivo from their metabolic stability in human liver microsomal preparations in vitro. *Drug Metab Dispos.* **26**:1120-1127.

Lee Y, Vassilakos A, Feng N, Lam V, Xie H, Wang M, Jin H, Xiong K, Liu C, Wright J, and Young A (2003) GTI-2040, an antisense agent targeting the small subunit component (R2) of human ribonucleotide reductase, shows potent antitumor activity against a variety of tumors. *Cancer Res.* **63**:2802-2811.

Lischda K, Starde D, Failing K, Herling A, Kramer W and Petzinge E (2003) Hepatobiliary elimination of bile acid-modified oligodeoxynucleotides in Wistar and TR-rats: evidence of mrp2 as carrier for oligonucleotides. *Biochem.Pharmacol*. **66**:565-577

Marcucci G, Stock W, Dai G, Klisovic RB, Liu S, Klisovic MI, Blum W, Kefauver C, Sher DA, Green M, Moran M, Maharry K, Novick S, Bloomfield CD, Zwiebel JA, Larson RA, Grever MR, Chan KK, and Byrd JC (2005) Phase I study of oblimersen sodium, an antisense to Bcl-2, in untreated older patients with acute myeloid leukemia: pharmacokinetics, pharmacodynamics, and clinical activity. *J.Clin.Oncol.* **23**:3404-3411.

McLure JA, Miners JO, and Birkett DJ (2000) Nonspecific binding of drugs to human liver microsomes. *Br.J Clin.Pharmacol.* **49**:453-461.

Noll BO, McCluskie MJ, Sniatala T, Lohner A, Yuill S, Krieg AM, Schetter C, Davis HL, and Uhlmann E (2005) Biodistribution and metabolism of immunostimulatory oligodeoxynucleotide CPG 7909 in mouse and rat tissues following subcutaneous administration. *Biochem.Pharmacol.* **69**:981-991.

Nolting A, DeLong RK, Fisher MH, Wickstrom E, Pollack GM, Juliano RL, and Brouwer KL (1997) Hepatic distribution and clearance of antisense oligonucleotides in the isolated perfused rat liver. *Pharm.Res.* **14**:516-521.

Downloaded from dmd.aspetjournals.org at ASPET Journals on April 8, 2024

DMD Fast Forward. Published on July 24, 2008 as DOI: 10.1124/dmd.108.021295
This article has not been copyedited and formatted. The final version may differ from this version.

Stein CA and Cheng YC (1993) Antisense oligonucleotides as therapeutic agents--is the bullet really magical? *Science* **261**:1004-1012.

Tang C, Lin Y, Rodrigues AD, and Lin JH (2002) Effect of albumin on phenytoin and tolbutamide metabolism in human liver microsomes: an impact more than protein binding. *Drug Metab Dispos.* **30**:648-654.

Tracy TS (2006) Atypical cytochrome p450 kinetics: implications for drug discovery. *Drugs R.D.* **7**:349-363.

Wei X, Dai G, Liu Z, Cheng H, Xie Z, Marcucci G, and Chan KK (2006a) Metabolism of GTI-2040, a phosphorothioate oligonucleotide antisense, using ion-pair reversed phase high performance liquid chromatography (HPLC) coupled with electrospray ion-trap mass spectrometry. *AAPS.J* **8**:E743-E755.

Wei X, Dai G, Marcucci G, Liu Z, Hoyt D, Blum W, and Chan KK (2006b) A specific picomolar hybridization-based ELISA assay for the determination of phosphorothioate oligonucleotides in plasma and cellular matrices. *Pharm.Res.* **23**:1251-1264.

Yu RZ, Geary RS, Monteith DK, Matson J, Truong L, Fitchett J, and Levin AA (2004) Tissue disposition of 2'-O-(2-methoxy) ethyl modified antisense oligonucleotides in monkeys. *J Pharm.Sci.* **93**:48-59.

Yu RZ, Zhang H, Geary RS, Graham M, Masarjian L, Lemonidis K, Crooke R, Dean NM, and Levin AA (2001) Pharmacokinetics and pharmacodynamics of an antisense phosphorothioate oligonucleotide targeting Fas mRNA in mice. *J.Pharmacol.Exp.Ther.* **296**:388-395.

Downloaded from dmd.aspetjournals.org at ASPET Journals on April 8, 2024

DMD Fast Forward. Published on July 24, 2008 as DOI: 10.1124/dmd.108.021295
This article has not been copyedited and formatted. The final version may differ from this version.

Footnotes

This study was supported by grants NCI R21 CA 105879 (G.M.) from the National Institutes of Health.

Address for reprint requests:

Kenneth K. Chan, Ph.D., Rm 308 OSU CCC, The Ohio State University, 410 West 12th Ave, Columbus, OH 43210, USA. Phone: 614-292-8294; FAX: 614-292-7766;

E-mail: chan.56@osu.edu

*Current address: Sanofi-Aventis US. Inc., Malvern, PA 19355, USA

Downloaded from dmd.aspetjournals.org at ASPET Journals on April 8, 2024

DMD Fast Forward. Published on July 24, 2008 as DOI: 10.1124/dmd.108.021295
This article has not been copyedited and formatted. The final version may differ from this version.

Legends for Figures:

Figure 1. A. Free fraction of GTI-2040 versus total concentration in human liver microsomes (0.2 mg/mL). **B**. Scatchard plot of bound GTI-2040 concentration versus bound to free GTI-2040 ratios in human liver microsomes.

Figure 2. A. Velocity of formation rate of 3'N-1 and 3'N-2 versus GTI-2040 substrate total concentrations plots in 0.3 U/mL of 3' exonuclease (Phosphodiesterase I) solution. **B**. Eadie-Hofstee plot of the kinetics of the sum of formation rate of 3'N-1 and 3'N-2 in 0.3 U/mL of 3' exonuclease (Phosphodiesterase I) solution.

Figure 3. A. Velocity of the sum of formation rate of 3'N-1 and 3'N-2 versus GTI-2040 substrate total concentrations in HLM (0.2 mg protein/mL). **B**. Eadie-Hofstee plot of the kinetics of the sum of formation rate of 3'N-1 and 3'N-2 in HLM (0.2 mg protein/mL).

Figure 4. A. Velocity of sum of formation rate of 3'N-1 and 3'N-2 versus unbound GTI-2040 substrate concentrations. **B**. Eadie-Hofstee plot of the kinetics of the sum of formation rates of 3'N-1 and 3'N-2 in HLM derived from unbound GTI-2040 (0.2 mg protein/mL).

Downloaded from dmd.aspetjournals.org at ASPET Journals on April 8, 2024

DMD Fast Forward. Published on July 24, 2008 as DOI: 10.1124/dmd.108.021295
This article has not been copyedited and formatted. The final version may differ from this version.

Table 1. Free fractions of GTI-2040 in human liver microsomes (0.2 mg protein/mL) and in human plasma (HPL).

Substrate concentration (μM)	Free fraction* (%) HLM	Free fraction* (%) HPL
0.1	7.2 ± 0.9	-[a]
0.2	10.4 ± 0.3	-[a]
0.5	22.4 ± 0.9	0.05±0.02
1	31.2 ± 7.1	0.09±0.06
2	32.9 ± 3.1	-[b]
5	35.4 ± 6.3	-[b]
10	63.5 ± 1.4	2.2±0.54
20	63.9 ± 2.7	-[b]
100	-[b]	5.5±2.3

[a]Results were below LLOQ of ELISA assay.
[b]Protein binding was not assessed in these concentrations.
Results are calculated from triplicate.

Downloaded from dmd.aspetjournals.org at ASPET Journals on April 8, 2024

DMD Fast Forward. Published on July 24, 2008 as DOI: 10.1124/dmd.108.021295
This article has not been copyedited and formatted. The final version may differ from this version.

Table 2. Kinetic parameters for the formation of 3'N-1 and 3'N-2 in 3' exonuclease (SVP) solution and in human liver microsomes.

Values	Phosphodiesterase I (0.3 U/ml)[a]	HLM (0.2 mg protein/mL)[a]	HLM (0.2 mg protein/mL)[b]
V_{max}	0.73 ± 0.06[b] nmole/hr	16.8 ± 8.0 nmole/hr/mg	16.5 ± 8.4 nmole/hr/mg
K_m (μM)	1.28 ± 0.42	12.1 ± 8.6	6.33 ± 3.2
n[c]	0.97 ± 0.05	1.28 ± 0.4	0.814 ± 0.09

[a]Results are presented as formation rates of sum of 3'N-1 and 3'N-2 vs total substrate concentrations. They were all determined in triplicate and from triplicate experiments.
[b]Results are presented as formation rates of sum of 3'N-1 and 3'N-2 vs unbound substrate concentrations, all from triplicate experiments.
[c]Hill coefficient

Downloaded from dmd.aspetjournals.org at ASPET Journals on April 8, 2024

Figure 1

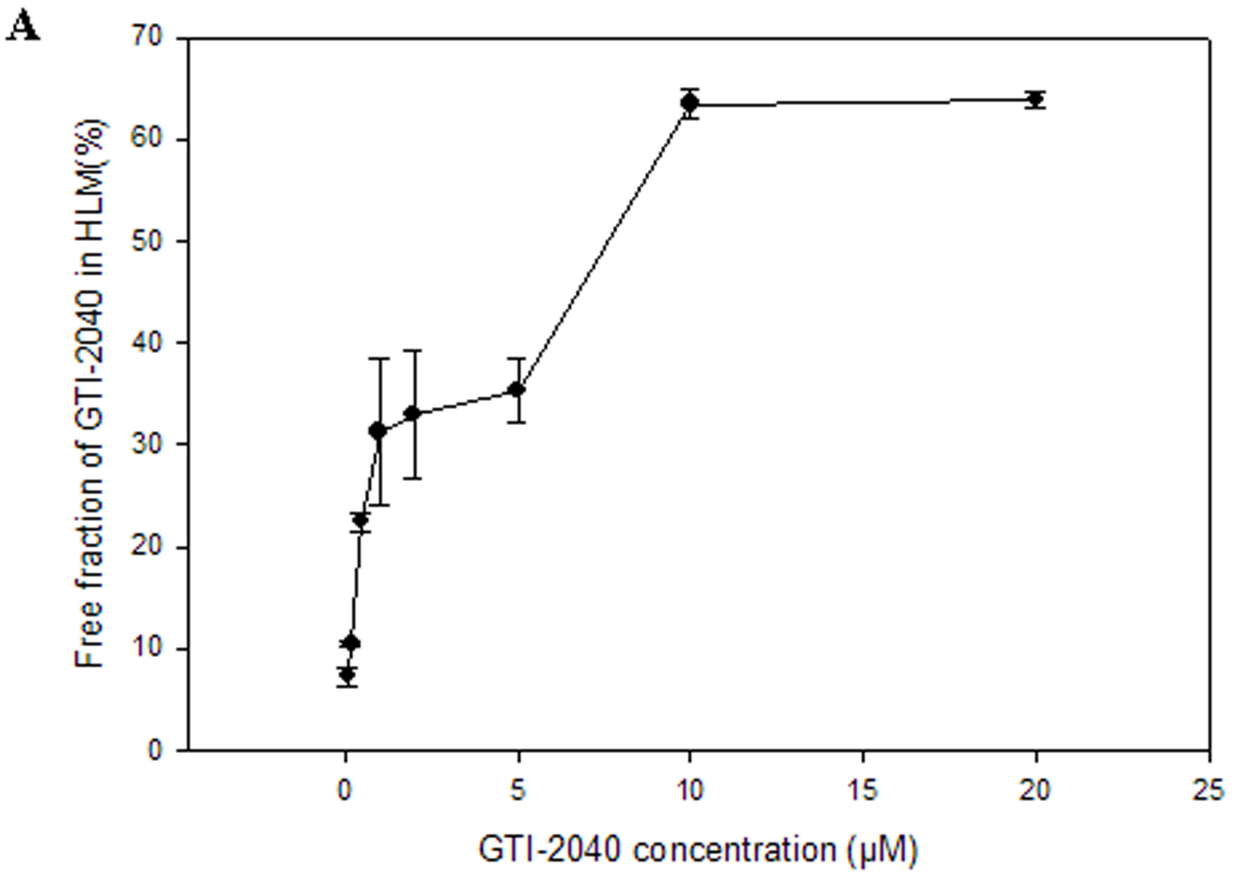
A
Free fraction of GTI-2040 in HLM(%)
0
10
20
30
40
50
60
70
0
5
10
15
20
25
GTI-2040 concentration (μM)

Figure 1

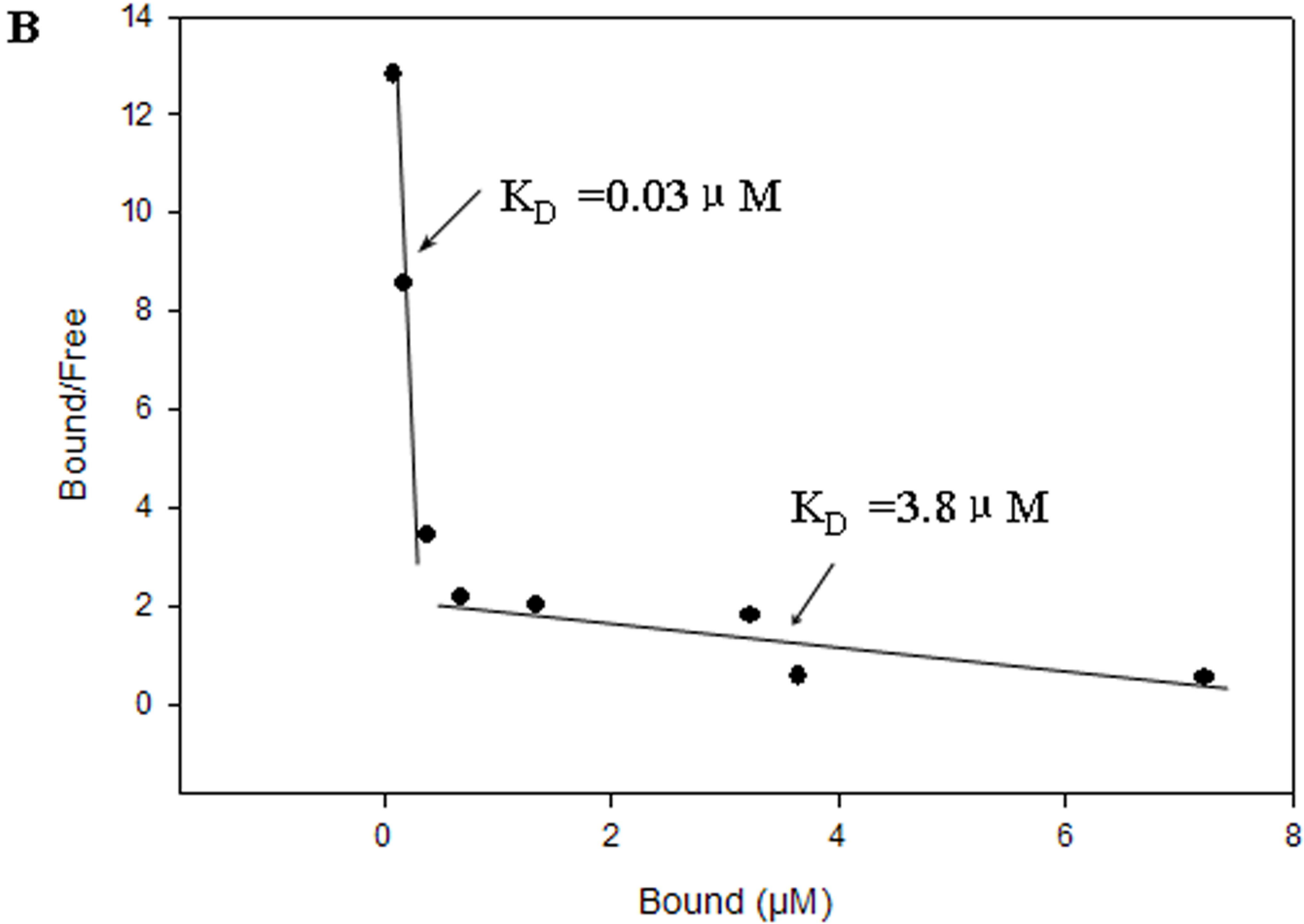

Figure 2

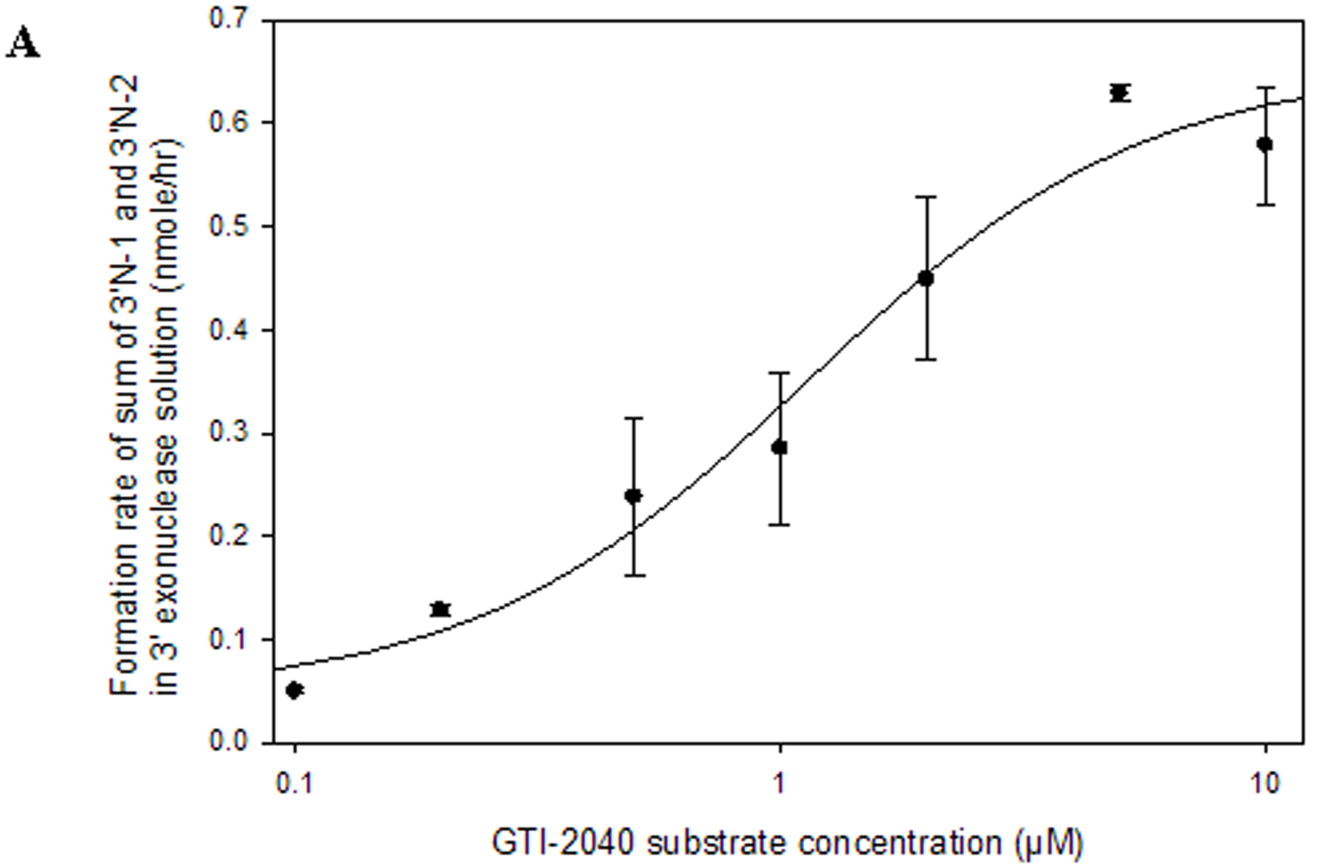
A
Formation rate of sum of 3'N-1 and 3'N-2 in 3' exonuclease solution (nmole/hr)
0.0
0.1
0.2
0.3
0.4
0.5
0.6
0.7
0.1
1
10
GTI-2040 substrate concentration (μM)

Figure 2

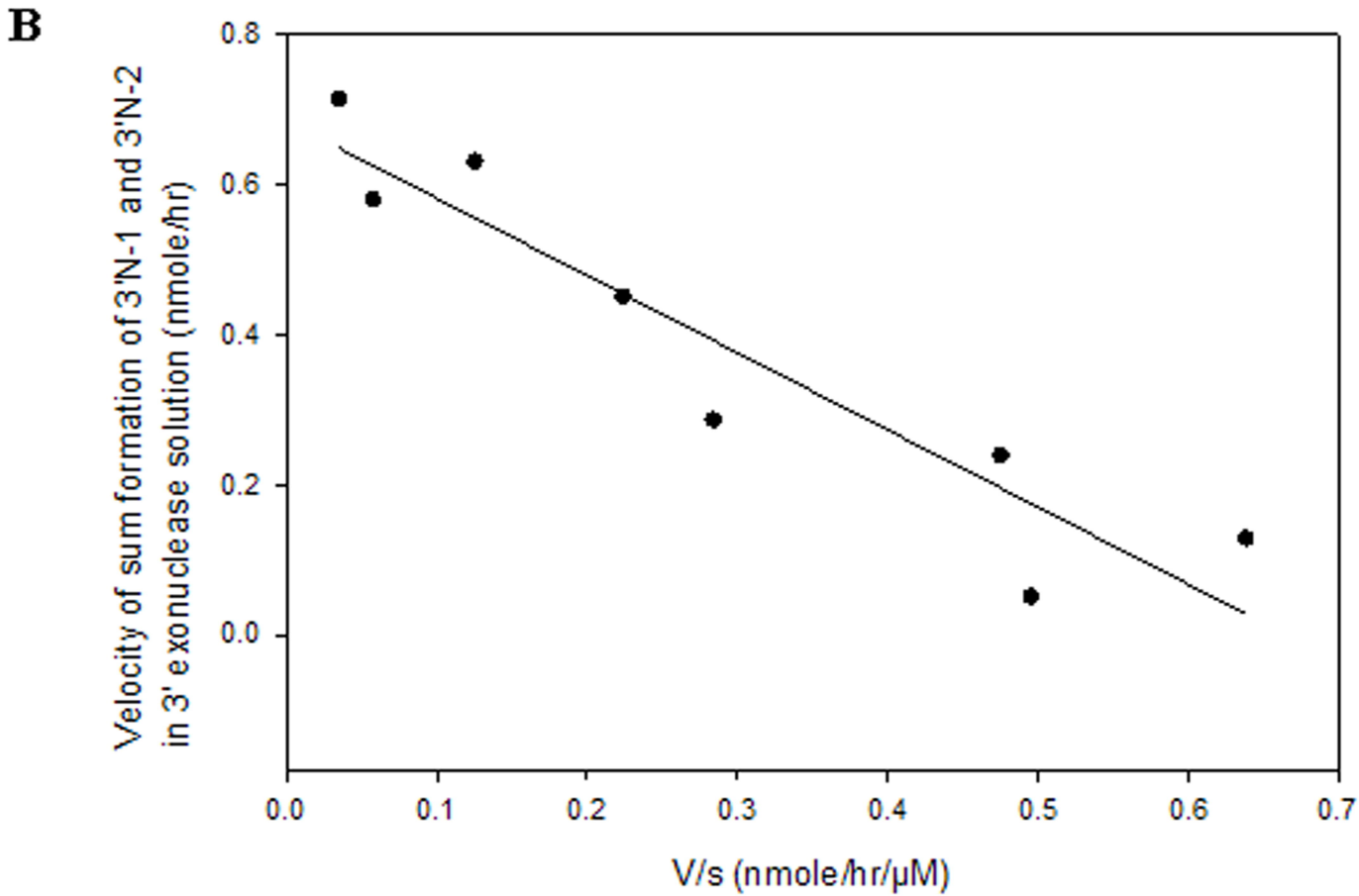
B
Velocity of sum formation of 3'N-1 and 3'N-2 in 3' exonuclease solution (nmole/hr)
0.8
0.6
0.4
0.2
0.0
0.0
0.1
0.2
0.3
0.4
0.5
0.6
0.7
V/s (nmole/hr/μM)

Figure 3

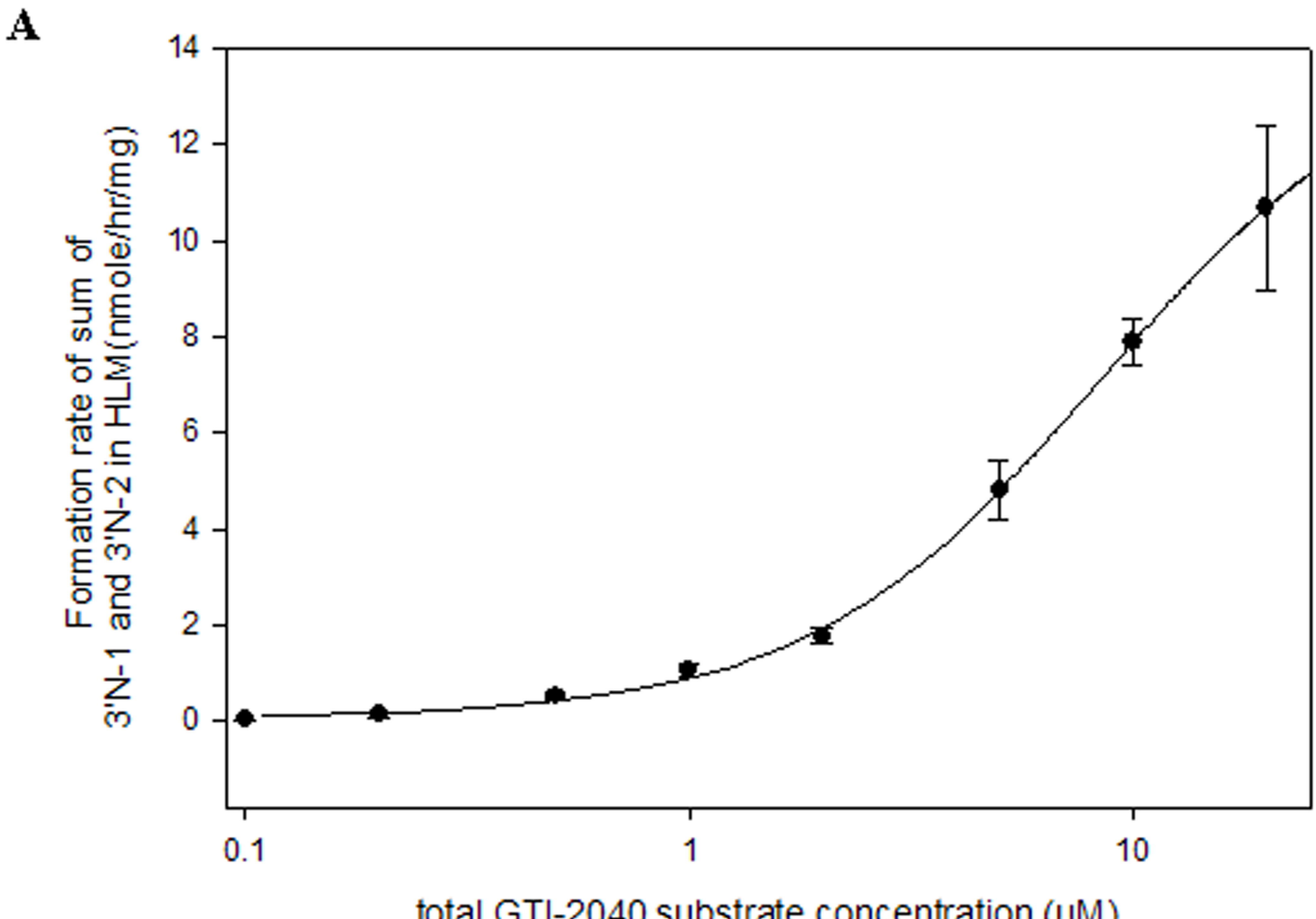
A
Formation rate of sum of
3'N-1 and 3'N-2 in HLM(nmole/hr/mg)
14
12
10
8
6
4
2
0
0.1
1
10
total GTI-2040 substrate concentration (μM)

Figure 3

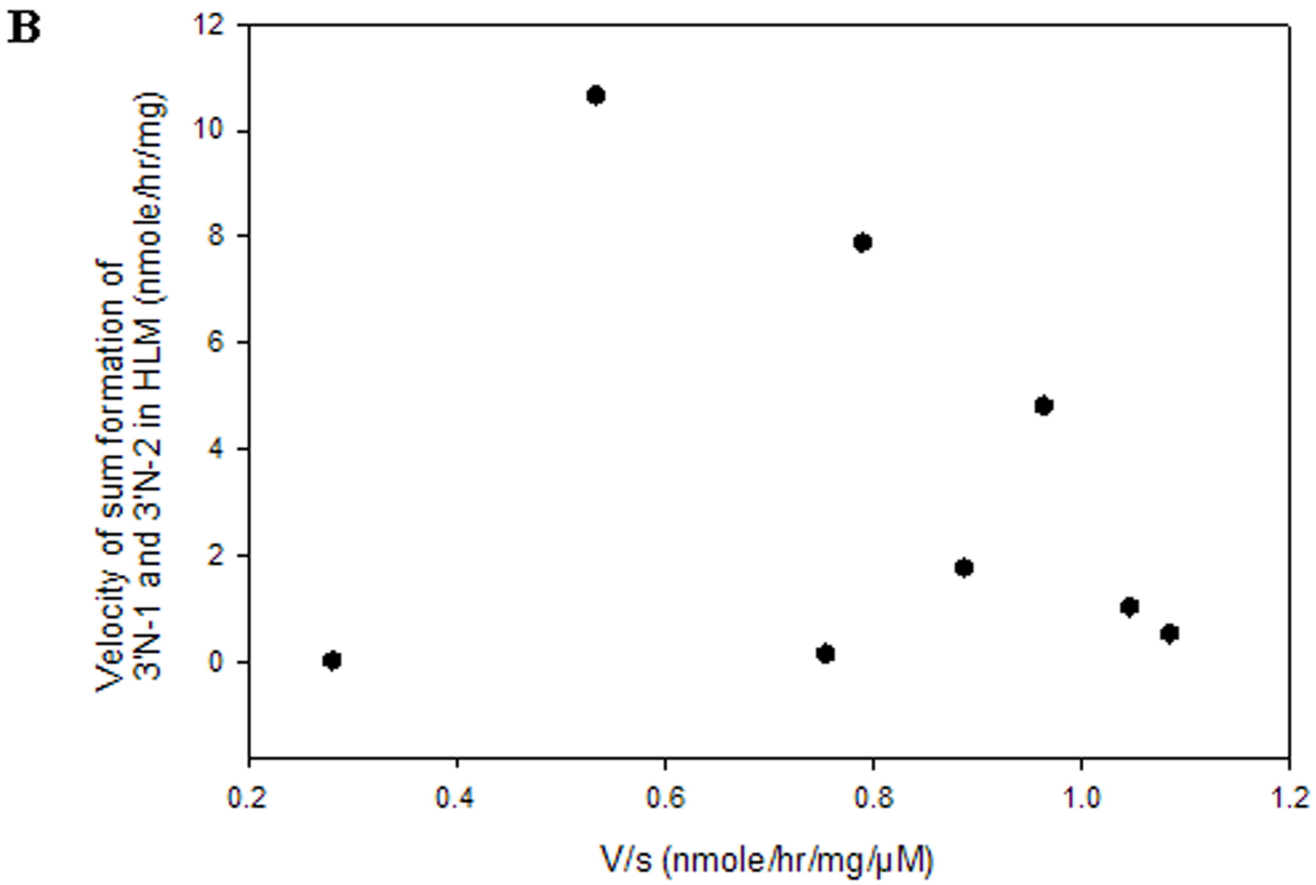
B
Velocity of sum formation of
3'N-1 and 3'N-2 in HLM (nmole/hr/mg)
12
10
8
6
4
2
0
0.2
0.4
0.6
0.8
1.0
1.2
V/s (nmole/hr/mg/µM)

Figure 4

A

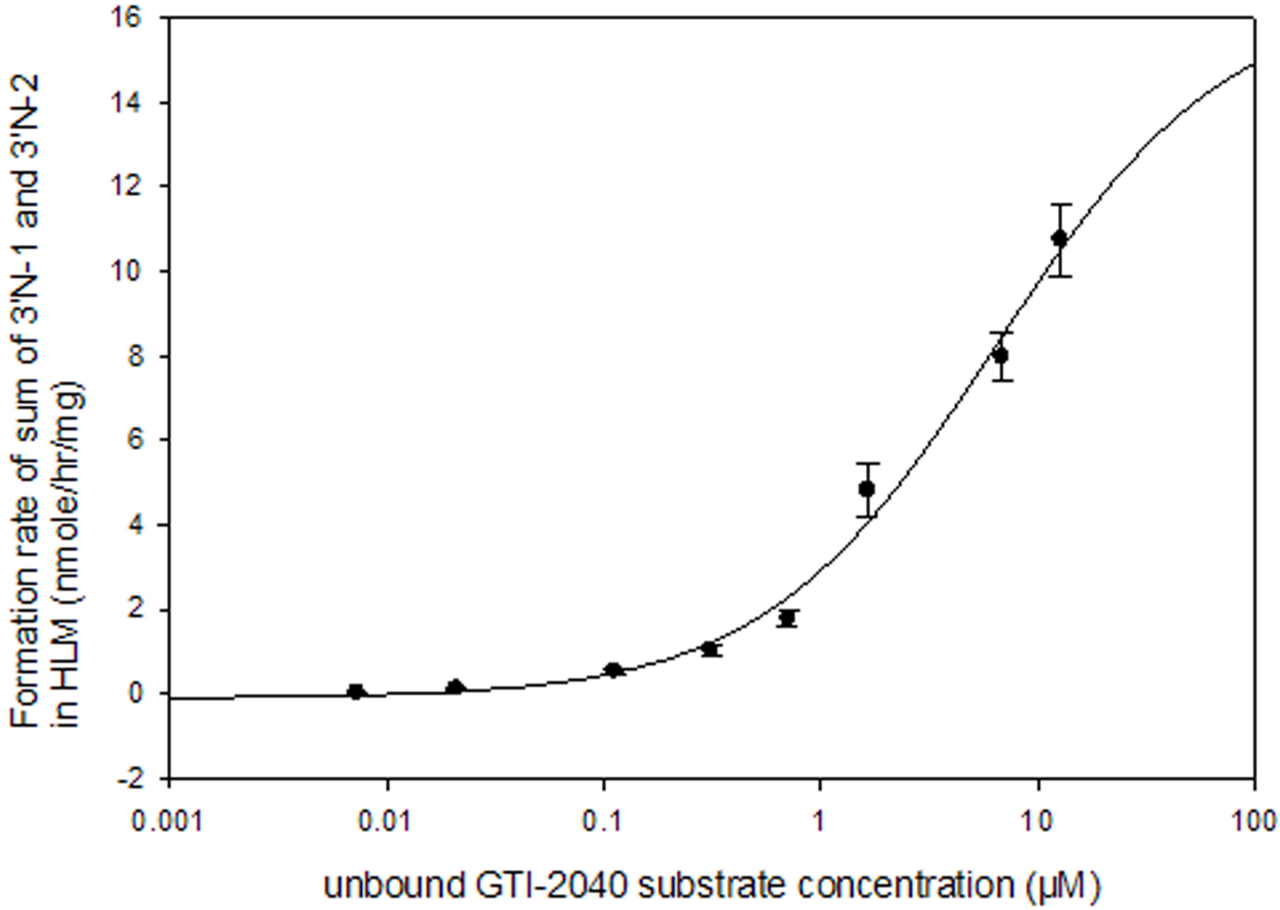
Formation rate of sum of 3'N-1 and 3'N-2 in HLM (nmole/hr/mg)
16
14
12
10
8
6
4
2
0
-2
0.001
0.01
0.1
1
10
100
unbound GTI-2040 substrate concentration (μM)

Figure 4